Transactions of the Canadian Society for Mechanical Engineering

Research Article

Performance analysis of a high-frequency two-stage proportional valve piloted by two high-speed on/off valve arrays

Qiang Gao[a,b], **Linfei Li**[a,c], **and Yuchuan Zhu**[a,c]

[a]Nanjing University of Aeronautics and Astronautics, Nanjing 210016, PR China; [b]National Research Center of Pumps, Jiangsu University, Zhenjiang 212013, PR China; [c]Wuxi Research Institute, Nanjing University of Aeronautics and Astronautics, Wuxi 214187, PR China

Corresponding author: **Yuchuan Zhu** (email: meeyczhu@nuaa.edu.cn)

Abstract

Two-stage proportional valves (TSPV) have been used extensively for electro-hydraulic control systems with large-flow applications. Due to the inherent characteristics of the pilot spool, such as hysteresis, motion quality, and dead zone, the dynamic performance of the traditional TSPV cannot be further improved. To solve this issue, this paper proposes a high-frequency two-stage proportional valve (HFTSPV) piloted by two high-speed on/off valve arrays, which integrates the advantages of dual nozzle flapper mechanism and parallel-connected valve technology. First, an entire mathematical model is established, in which some key parameters are estimated by experiments, such as the actual diameters and flow coefficients of orifices, and flow coefficient of pilot valve. Then, the influences of fixed orifices with different diameters on the dynamic characteristics of main spool are explored. Subsequently, the optimal diameter of fixed orifice is calculated theoretically by using the maximum pressure sensitivity and flow linearity, aiming to realize the high dynamic and small displacement fluctuation. Finally, step and sinusoidal tracking experiments show that the delay time of the HFTSPV is close to 3.3 ms, and the displacement fluctuation decreases with the increase of tracking frequency. Amplitude–frequency results indicate that −3 dB frequency of the HFTSPV reaches 16 Hz under ±50% full scale and 30 Hz under 0%–50% full scale.

Key words: high-frequency proportional valve, high-speed on/off valve array, dual nozzle flapper, parallel-connected digital valve technology, dynamic performance

1. Introduction

In fluid power transmission field, hydraulics is used for the generation, control, and transmission of power by using the pressurized liquids (Yang and Pan 2015), such as oil or water. Electro-hydraulic proportional control system plays an important role in the last 40 years by virtue of its advantages, such as good dynamic response and high precision, in which proportional valve serves as the core control component. The two-stage proportional valves (TSPV) have been extensively used for electro-hydraulic control systems with large-flow applications, such as excavator hydraulic system (Zhong et al. 2022), landing gear retraction system (Yin et al. 2016), and electro-hydraulic lifting system (Hou et al. 2017). The pilot stage of the TSPV is used to amplify the electrical actuator signal to move the main valve (Xu et al. 2016), which means the pilot valve is the key to achieving the increased reliability, fast speed, and digital intelligence of the TSPV.

Nowadays, some structures such as spool valve actuated by proportional solenoid and dual nozzle-flapper structure are usually applied to be the pilot stage for the traditional TSPV (Nie et al. 2018; Wang et al. 2020; Zhang et al. 2023). However, for the former, the dynamic performance and big flow rate of the pilot proportional valve cannot be simultaneously obtained because of some disadvantages, such as hysteresis caused by the coil inductance, high motion inertia of the spool, high friction, leakage, and structural dead zone; for the latter, the dynamic performance and big flow rate are both achieved but at the expense of reliability and cost due to poor zero stability, high machining tolerance, and micron-level fit tolerance. To overcome the nonlinearity, low dynamic response, and rough precision caused by the dead-zones in the traditional pilot proportional spool, a cascade dead-zones inverse method based on gain estimation, and dead-zone detection was proposed to improve the linearity of main valve (Xu et al. 2017). Moreover, two independent 2/3 type spools are used to be the pilot stage instead of traditional 3/4 type spool, which is beneficial to improve the dynamic performance (Zhang et al. 2019). However, due to the inherent defects of the pilot spool, the dynamic performance and reliability cannot be further improved.

Recently, taking high-speed on/off valve (HSV) as the pilot stage seems to be another effective way to enhance the

response speed of two-stage electro-hydraulic proportional valve. There are several reasons for this (Gao et al. 2022): (a) HSV only works in fully open or closed states, so it almost has no leakage; (b) reliability of signal transmission is higher than that of the traditional proportional valve because HSV is controlled by digital signal; (c) machining tolerance between the valve and sleeve in HSV is bigger than that of the traditional spool, which makes the HSV low cost and insensitive to oil contamination. For example, Zeng et al. (2015) designed a pilot stage composed of four HSVs for the directional valve. In this research, some factors such as pulse width modulation (PWM) signal, coil current, HSV's displacement, and main spool's displacement are analyzed by AMESim simulation. In the study of reference (Zhong et al. 2021), a programmable valve with digital valve controlled pilot stage was proposed in which the main spool controlled by two 2/3 HSVs exhibited poor dynamic performance because of the flow restriction of the pilot HSV. Tamburrano et al. (2020) designed a novel two-stage servo valve, which is piloted by two small piezoelectric-driven valves. In this study, experiments show that the opening and closing time of the pilot valve are within 5 ms. A digital proportional valve that is piloted by a combination of two fixed orifices and two HSVs was developed (Gao et al. 2021) in which the moving speed of the main spool should be improved by increasing the flow rate of the pilot HSV.

Compared to HSV with big flow rate, the parallel-connected digital valve technology can increase the flow rate and maintain the same dynamic performance at the same time, which is considered to be a solution instead of the proportional technology (Brandstetter et al. 2017; Pan and Plummer 2018). Linjama has carried out a lot of research work about this technology, and proved the effectiveness of this technology in reliability and efficiency through simulation and experiments. Linjama proposed a new structure named Digital Flow Control Unit (DFCU) that is composed of several on/off valves (Laamanen et al. 2003; Lantela and Pietola 2017). A high-flow miniature digital valve system composed of four DFCUs is designed in reference Paloniitty (2018), which is used to replace the standard proportional valve. Paloniitty and Linjama (2018) successively designed a digital water valve system in which the system consists by a plurality of on/off valves to improve the output flow rate. To reduce the whole size of digital valve package, vacuum brazed steel–copper laminate technology is used. A high-frequency proportional flow control valve with pilot switching valve was proposed in which a valvistor poppet valve is taken as the main stage (Xiong and Huang 2018; Wang et al. 2021). In this research, the effects of the PWM duty ratio, PWM frequency, number of switching valves, and pressure drop on the performance of the main stage are analyzed by simulations and experiments. To improve the control precision and switching uniformity of the parallel-connected digital valves, Wang et al. (2023) proposed an equivalent continuous metering method with a uniform switching strategy. In reference Li et al. (2023), several on/off valves arranged in a row are used to control the braking pressure for aircraft, and an antidisturbance slip ratio strategy was presented to realize the high precision control of the braking pressure.

A novel high-frequency two-stage proportional valve (HFTSPV) piloted by two high-speed on/off valve arrays (HSVAs) is proposed in this research. The design ideal of the proposed HFTSPV is inspired by the traditional dual nozzle flapper structure, and fully integrates the advantages of parallel-connected digital valve technology. This paper is organized as follows. Section 2 gives the working principle and the mathematical model of the proposed HFTSPV. Section 3 shows the parameters identification. Analysis and optimization of the orifice's diameter are carried out in Section 4. Section 5 gives the step tracking, sinusoidal tracking, and amplitude–frequency tracking experiments. The important conclusions can be found in Section 6.

2. Operating principle and modeling of HFTSPV

Inspired by the working mechanism of dual nozzle flapper structure, an HFTSPV piloted by two HSVAs is designed, as exhibited in Fig. 1. The proposed HFTSPV consists of a pilot stage and a main stage. The pilot stage consists of two HSVAs (HSVA-A and HSVA-B) and two fixed orifices. Each HSVA consists of three HSVs with same flow structure, which are installed in parallel.

As shown in Fig. 1, for the proposed pilot stage, the two HSVAs are independently driven by digital signals, which is different from the coupling control in traditional double nozzle flapper valve. In addition, the HSV only works in fully open or fully closed states, which makes the HSV insensitive to oil contamination and low throttling loss. Therefore, the advantages of the proposed HFTSPV includes high reliability, high efficiency, and more control freedom. The proposed HFTSPV has three working states:

a) Middle working mode: the pilot HSVA-A and HSVA-B are de-energized, both chamber A and chamber B are connected to the oil supply through fixed throttling orifices so that the pressure in chamber A and chamber B is the same, which results in the main spool being held in middle position by the centering spring.
b) Right working mode: the pilot HSVA-A is de-energized and the HSVA-B working in switching mode by exciting voltage, leading that chamber B connects to the tank. Then, the pressure in the chamber B starts to decrease and is smaller than that in the chamber A, which causes that the main spool moves to the right side under the action of pressure difference between chamber A and chamber B.
c) Left working mode: the pilot HSVA-B is closed and the HSVA-A working in switching mode by exciting voltage, leading that chamber A connects to the tank. Then, the pressure in the chamber A starts to decrease and is smaller than that in the chamber B, which causes that the main spool moves to the left side under the action of pressure difference between chamber A and chamber B.

Fig. 1. Schematic diagram and structure of the proposed high-frequency two-stage proportional valve. HSVA, high-speed on/off valve array.

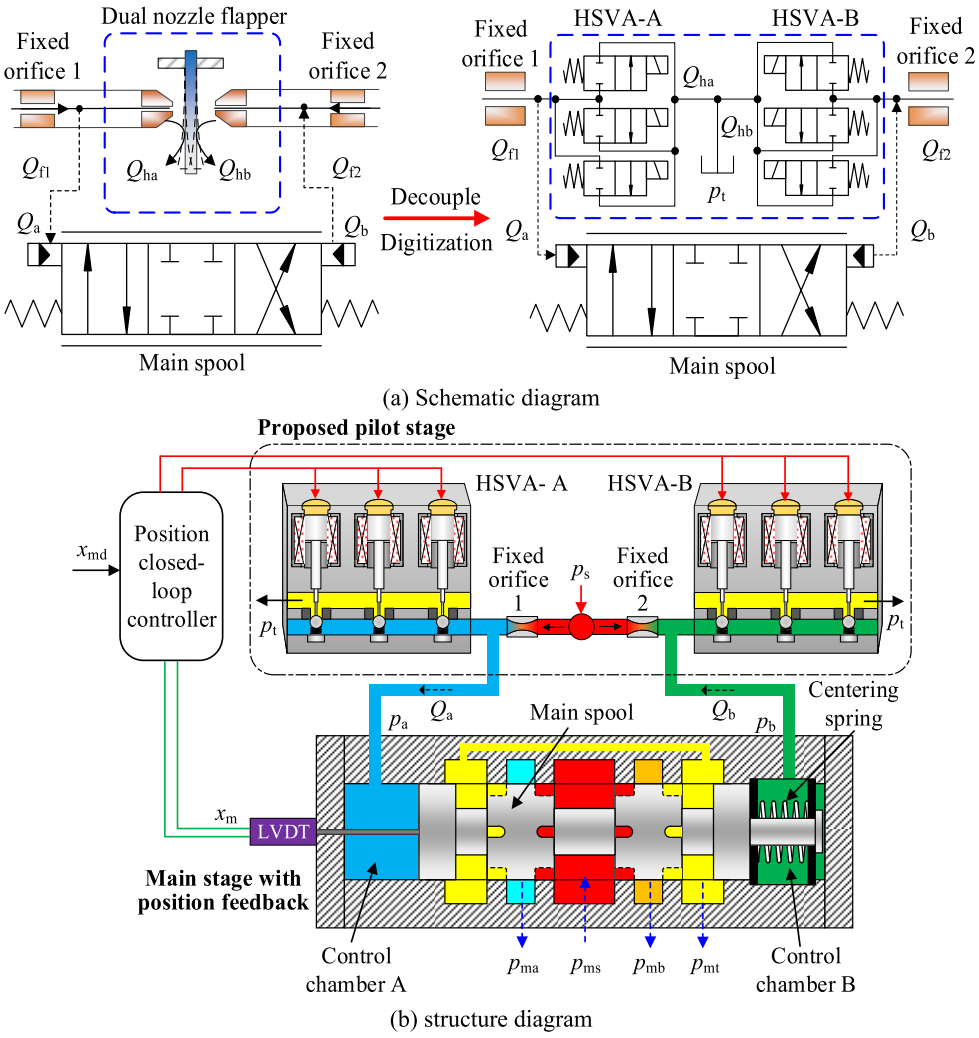

It can be seen that the high precision control of the main spool's position can be realized by alternately controlling the working state of the pilot HSVA-A and pilot HSVA-B.

2.1. Modeling of the pilot stage

The flow rates across the two orifices with same structure in the pilot stage are defined as

$$(1)\quad Q_{pf1} = C_{pf}A_{pf}\sqrt{\frac{2(p_{ps}-p_{ma})}{\rho}} = C_{pf}\frac{\pi d_{pf}^2}{4}\sqrt{\frac{2(p_{ps}-p_{ma})}{\rho}}$$

$$(2)\quad Q_{pf2} = C_{pf}A_{pf}\sqrt{\frac{2(p_{ps}-p_{mb})}{\rho}} = C_{pf}\frac{\pi d_{pf}^2}{4}\sqrt{\frac{2(p_{ps}-p_{mb})}{\rho}}$$

where Q_{pf1} and Q_{pf2} are the flow rates across the pilot orifice 1 and pilot orifice 2, p_{ps} is the pilot supply pressure, p_{ma} and p_{mb} are the control pressure in chamber A and chamber B of the main spool, C_{pf}, d_{pf}, and A_{pf} are the flow coefficient, diameter, and opening area of the pilot orifice; ρ is the density of oil.

Since the pilot HSVA-A and pilot HSVA-B have same structure, ignoring the machining error, the flow rate of pilot HSVA-A and pilot HSVA-B can be defined as

$$(3)\quad Q_{ha} = n_{ha}C_hA_{hmax}\sqrt{\frac{2(p_{ma}-p_t)}{\rho}}$$

$$(4)\quad Q_{hb} = n_{hb}C_hA_{hmax}\sqrt{\frac{2(p_{mb}-p_t)}{\rho}}$$

where Q_{ha} and Q_{hb} are the output flow rates of the pilot HSVA-A and HSVA-B, p_t is the tank pressure, C_h is the flow coefficient of the HSV, n_{ha} and n_{hb} are the number of valves open in pilot HSVA-A and pilot HSVA-B, and A_{hmax} is the maximum flow area of the HSV.

The relationship between the HSV's flow area and the command signal (PWM signal) is often used to describe the dynamic characteristic of the HSV, as shown in Fig. 2. In Fig. 2, t_{od}, t_{om}, t_{to}, t_{cd}, t_{cm}, and t_{tc} are the opening delay time, opening movement time, total opening time, closing delay time,

Fig. 2. Relationship between high-speed on/off valve's opening area and command signal.

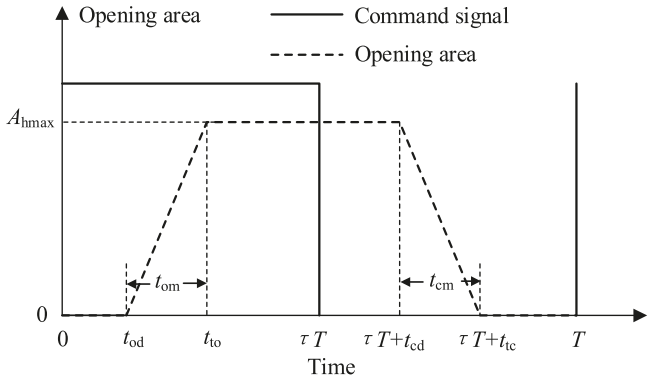

closing movement time, and total closing time, respectively. T denotes the period of the PWM signal.

As shown in Fig. 2, the opening delay time and the closing delay time of the HSV are easily affected by the coil inductance and mechanical hysteresis. The opening movement time and the closing movement time relate to the electromagnetic force and the moving mass. To accurately describe the motion state of the HSV, the transmission delay module and the speed limiter module in the MATLAB/Simulink software are used to simulate the opening delay characteristics, closing delay characteristics, opening motion characteristics, and closing motion characteristics of HSV.

2.2. Modeling of the main stage

According to the flow continuity equation, the flow rate across the chambers A and B of the main spool can be written as

$$Q_{ma} = Q_{pf1} - Q_{ha} \tag{5}$$

$$Q_{mb} = Q_{hb} - Q_{pf2} \tag{6}$$

Ignoring the main spool's leakage, the pressure in the chambers A and B are defined by

$$\frac{dp_{ma}}{dt} = \frac{\beta_e}{V_m + A_m x_m}\left(Q_{ma} - A_m \frac{dx_m}{dt}\right) \tag{7}$$

$$\frac{dp_{mb}}{dt} = \frac{\beta_e}{V_m - A_m x_m}\left(A_m \frac{dx_m}{dt} - Q_{mb}\right) \tag{8}$$

where V_m is the initial volume of the chambers A and B, A_m is the end surface area of the main valve, β_e is the fluid bulk modulus, and x_m is the displacement of the main spool.

Based on the Newton's second law, the dynamic model of the main spool is

$$m_m \frac{d^2 x_m}{dt^2} = (p_{ma} - p_{mb})A_m - k_m x_m - F_{mp} - B_m \frac{dx_m}{dt} - F_{mc} - F_{ms} \tag{9}$$

where m_m is the mass of the main spool, B_m is the viscous friction coefficient of the main spool, k_m and F_{mp} are the stiffness and preload force of the centering spring, and F_{mc} and F_{ms} are the coulomb friction force and steady flow force acting on the spool.

The steady flow force F_{ms} can be written as

$$F_{ms} = 2C_{mv}C_{md}\cos\theta_m \sum_{k=1}^{4}(A_k \Delta p_k) \tag{10}$$

where A_k is the opening area of the variable orifice distributed on spool shoulder, Δp_k is the pressure difference across the variable orifice, C_{mv} and C_{md} are the fluid velocity coefficient and flow coefficient of main spool, and θ_m is the fluid jet angle of the variable orifice.

The opening areas of these variable orifices distributed on main spool's shoulder are defined as (Gao et al. 2024)

$$A_k = f(n, R_{mk}, x_{m0}) = \begin{cases} nR_{mk}^2\left[\arccos\left(1 - \frac{x_{m0}}{R_{mk}}\right) - \left(1 - \frac{x_{m0}}{R_{mk}}\right)\sqrt{\frac{x_{m0}}{R_{mk}}\left(2 - \frac{x_{m0}}{R_{mk}}\right)}\right], & 0 \le x_{m0} \le R_{mk} \\ \frac{\pi n R_{mk}^2}{2} + 2nR_{mk}(x_{m0} - R_{mk}), & R_{mk} < x_{m0} \end{cases} \tag{11}$$

where n, R_{mk}, and x_{m0} denote, respectively the number, radius, and opening of these circular ports around the main spool.

2.3. Simulation model

According to eqs. 1–11, the simulation model of the HFT-SPV is built by MATLAB/Simulink, as shown in Fig. 3. The main parameters are given in Table 1.

According to Table 1, except for the flow coefficient of the orifice and the HSV, most of the parameters' value of the proportional valve are already given.

3. Parameters identification

3.1. Diameter and flow coefficient of fixed orifice

The flow characteristic of the fixed orifices integrated into the pilot stage affects the response of the pilot pressure. To obtain the flow coefficients of different types of fixed orifices, and considering the machining error of the orifice, the diameters of these orifices in this study need to be tested firstly. In this study, an optical microscope (Shenzhen aosvi optical instrument, HD228SD) is used to observe and calibrate the diameters of different types of orifices. The test system and test results are presented in Fig. 4.

Fig. 3. MATLAB/Simulink simulation model for the proposed valve. HSVA, high-speed on/off valve array.

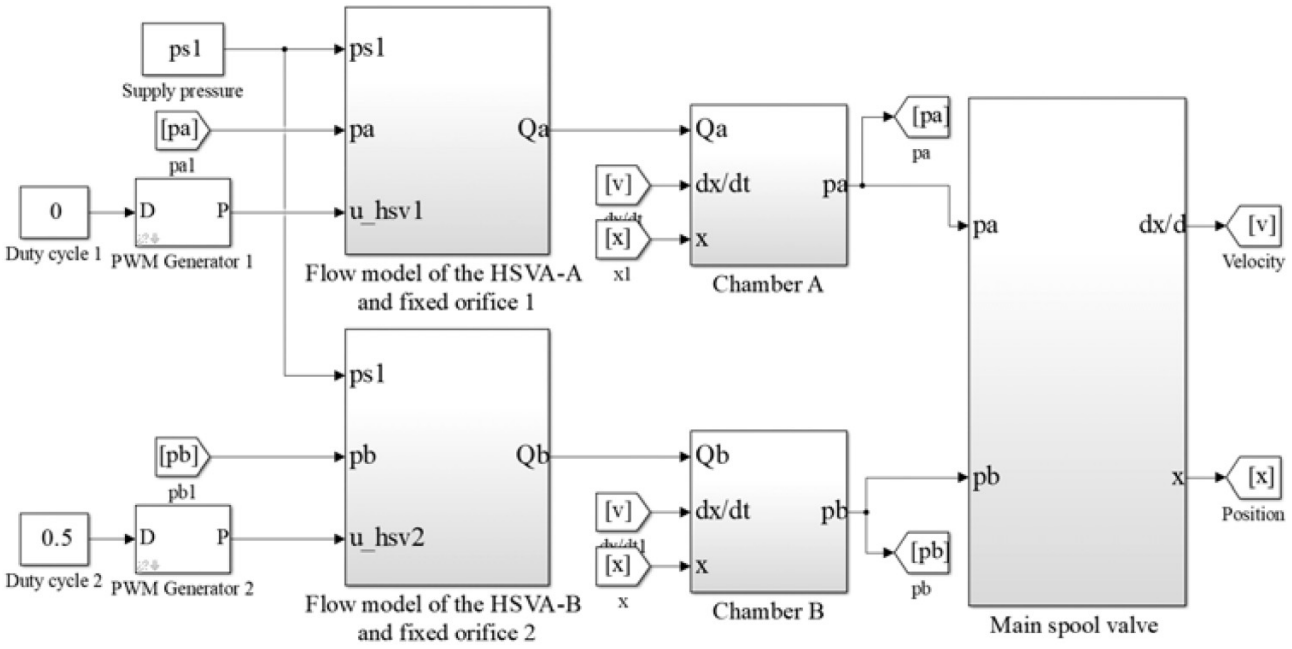

Table 1. Main parameters of the proposed high-frequency two-stage proportional valve.

Parameter	Value
Maximum opening area of pilot HSV, A_{hmax}/(mm^2)	1.024
Radius of circular port, R_{mk}/(mm)	1
Viscous friction coefficient, B_m/(N/(m/s))	17.6
Coulomb friction force, F_{mc}/N	8
Initial volume of chamber A, V_{a0}/(mm^3)	3750
Initial volume of chamber B, V_{b0}/(mm^3)	3750
Center dead-band of main spool, Δ/(mm)	0.62
Cross-section area of main spool, A_m/(mm^2)	314
Main spool's spring preload, F_{mp}/(N)	50
Moving mass of the main spool, m_m/(g)	205
Centring spring stiffness, k_m/(N/mm)	50
Flow coefficient of main spool, C_{md}	0.61
Fluid velocity coefficient of main spool, C_{mv}	0.98

Note: HSV, high-speed on/off valve.

According to Fig. 4, there indeed exists errors between the test results and standard values of the fixed orifices' diameter. When the standard diameter of the orifice is 0.6 mm, the maximum error can reach 10.8%, and the errors of the other specifications of orifices are within 3.5%. Moreover, according to the observation of the microscopic morphology, it can be found that there is a certain roundness error in the small hole, and the roughness of the edge processing is relatively large.

Based on the actual values of the orifices' diameter and the measurements of the flow rate of different standard orifices, the flow coefficients of these orifices can be estimated based on the least square method. Comparisons between the estimation and the test of the orifices' flow characteristic are shown in Fig. 5.

Figure 5 indicates that the flow coefficients of different types of fixed orifices (0.4, 0.6, 0.8, 1.0, and 1.2 mm) are 0.75, 0.75, 0.86, 0.76, and 0.85, respectively. The flow fitting curves are basically consistent with the experimental data, and the accuracy of the established orifice plate flow model is verified.

3.2. Flow coefficient of HSV

When six HSVs are simultaneously driven by the drive board, each valve cannot reach the maximum opening due to insufficient power of the drive board. To simplify the analysis, the influence of the driving board on the HSVs is ignored. It is assumed that the opening of the HSV always reaches the maximum position, the flow coefficient of the HSV changes and is determined by experiment. In addition, due to the processing and assembly errors, and inconsistent service time of each HSV, the flow coefficient of each HSV is different. In experiment, each HSV is controlled to open separately, then the flow coefficient of each HSV is estimated by least square method on the basis of the experimental results of the main spool's position, as shown in Fig. 6.

It is manifest from Fig. 6 that the flow coefficients of the six HSVs (HSV-1 to HSV-6) are 0.265, 0.265, 0.278, 0.330, 0.278, and 0.295, respectively. The simulation results of the main spool's displacement are basically consisted with the experimental results, which prove the accuracy of the simulation model. Moreover, the dynamic characteristics and flow characteristics of the six HSVs have certain errors. There are two reasons for this: one is that the length of the air gap changes due to machining error and assembly error in the production and assembly; the other is that the service time of each HSV is different, which causes the inconsistent wear of valve port.

Fig. 4. Testing system of the orifices based on an optical microscope.

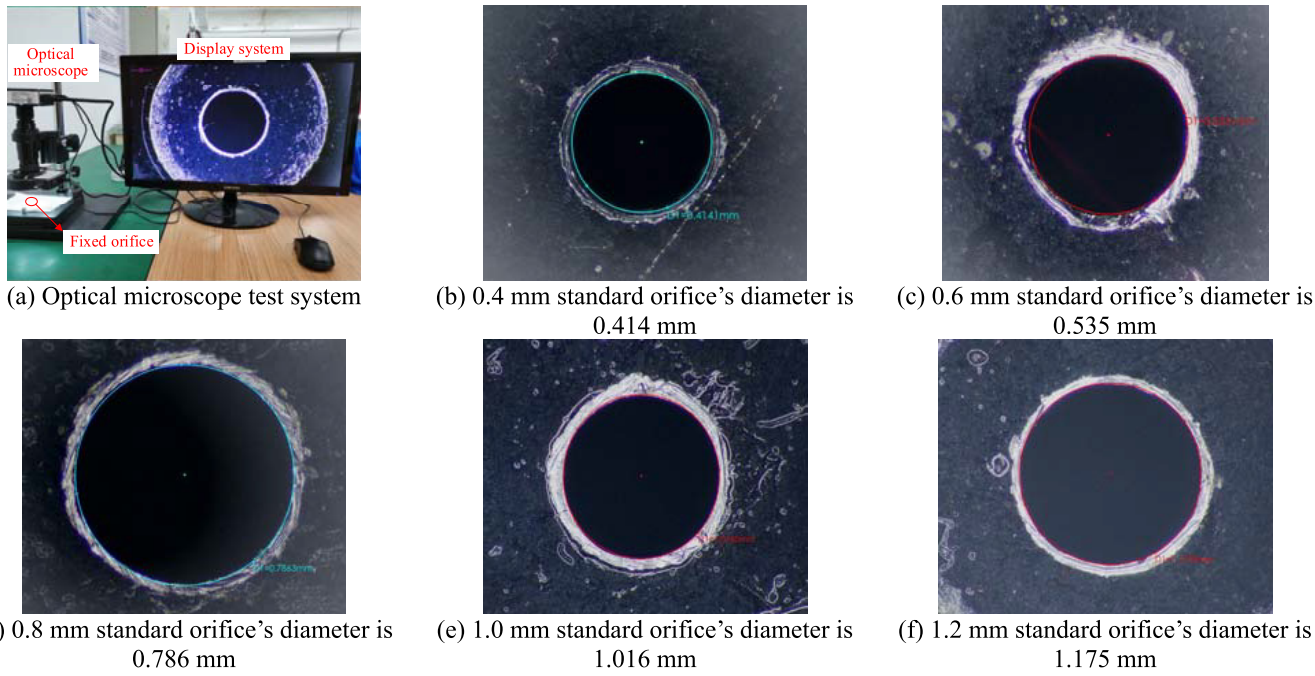

(a) Optical microscope test system

(b) 0.4 mm standard orifice's diameter is 0.414 mm

(c) 0.6 mm standard orifice's diameter is 0.535 mm

(d) 0.8 mm standard orifice's diameter is 0.786 mm

(e) 1.0 mm standard orifice's diameter is 1.016 mm

(f) 1.2 mm standard orifice's diameter is 1.175 mm

Fig. 5. Estimation and test results of orifices' flow characteristic.

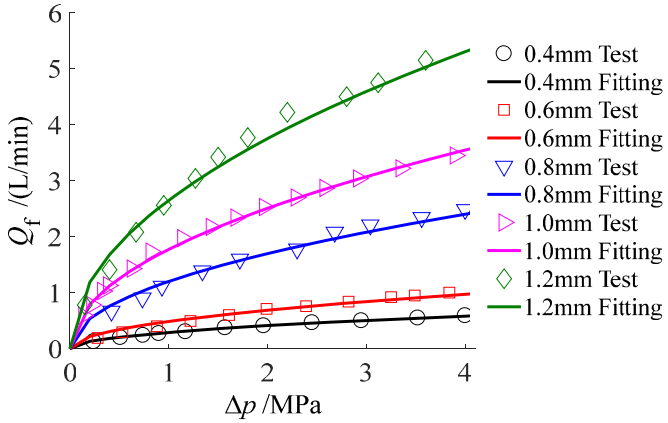

4. Design method of orifice's diameter

4.1. Influences of orifice's diameter on the main spool

To quantitatively analyze the influence of the orifice's diameter on the main spool' displacement, the dynamic response of the displacement under different orifices' diameter are obtained through simulations, as shown in Fig. 7, where the duty cycle τ is 0.5 and 1.

As shown in Fig. 7, when the duty cycle is 0.5, as the orifice's diameter gradually increases, the flow rate into the control chamber increases, which leads to the increase of the main spool's displacement during the high voltage level. Since the oscillation amplitude of the main spool's displacement is larger, the effective movement first increases and then decreases. When the duty cycle is 1, it means that the HSVs work in fully open state. By observing the main spool's displacement curves under different orifices' diameter, it is easy to find that when the diameter of the orifice is in the range of 0.4–1.0 mm, the larger the diameter, the faster the main spool's displacement rises. However, when the orifice's diameter reaches 1.2 mm, the rising speed of the spool displacement decreases instead.

In summary, the increase of the orifice's diameter during the range of 0.4–1 mm is beneficial to improve the dynamic response of the main spool, but it will cause the oscillation of the main spool displacement. Therefore, it is necessary to optimize the size of the orifice's diameter to make the main spool displacement take into account the characteristics of high dynamic and small fluctuation.

4.2. Design method of orifice's diameter

The ideal of the HFTSPV is derived from the traditional dual nozzle flapper's structure that the HSVA is taken as the nozzle, as shown in Fig. 8.

Figure 8 indicates that the two orifices are applied to generate pressure in chamber A and chamber B, which is regulated by controlling the PWM duty cycles. When the pilot HSVA is controlled by PWM signal, the initial duty cycle is applied to simulate the flapper's null position. Since the structure parameters of the pilot HSV used in this work are known to improve the dynamic characteristics and linear controllability of the digital pilot stage, the orifice size of the digital pilot stage needs to be optimized with the goal of control sensitivity and flow accuracy.

To analyze the maximum control pressure sensitivity of the proposed pilot stage, the corresponding flow equations are

Fig. 6. Identification of the flow coefficient of each high-speed on/off valve (HSV).

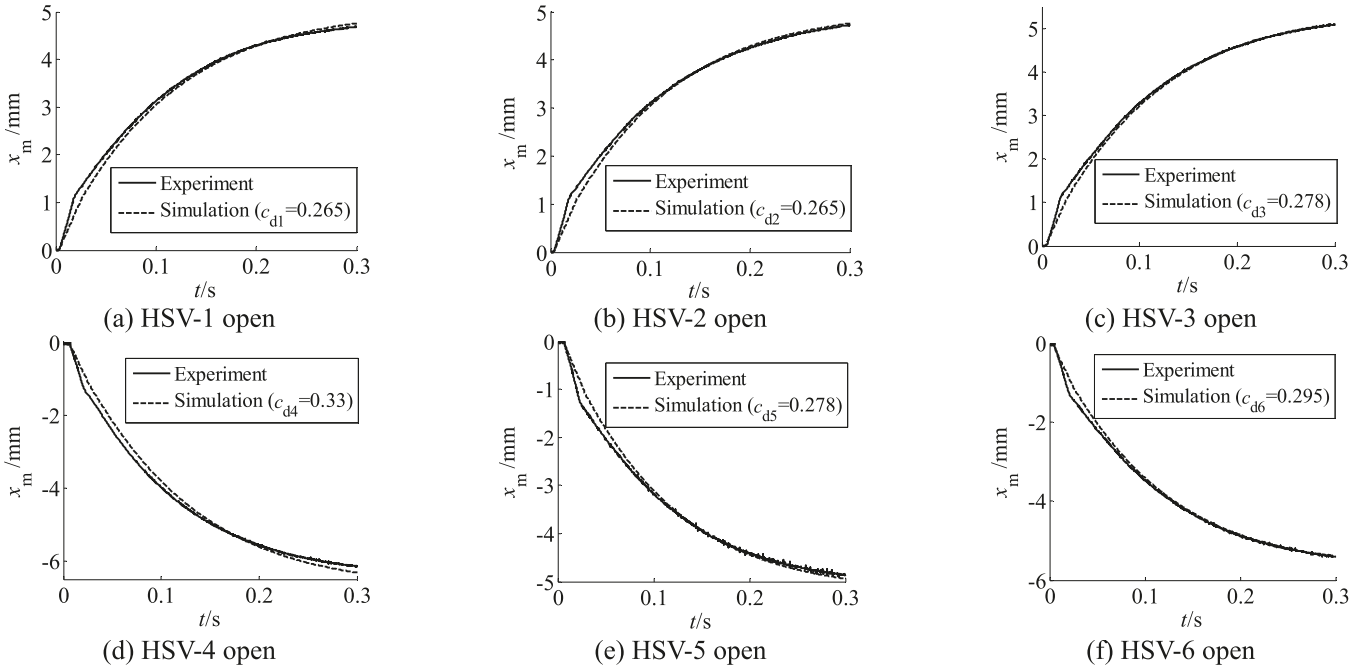

Fig. 7. Influences of the orifice's diameter on the displacement of the main spool.

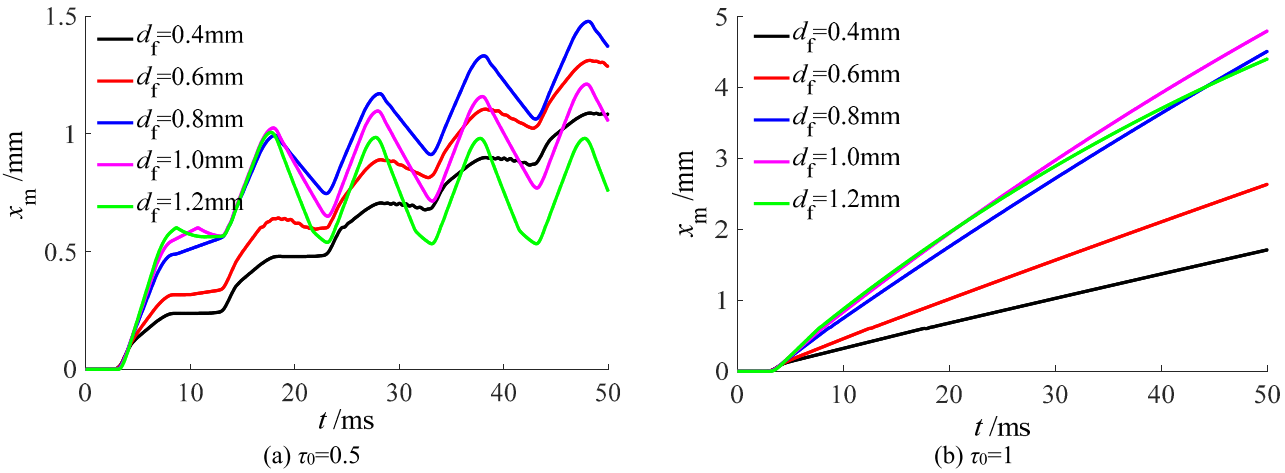

Fig. 8. Relationship between the dual nozzle-flapper's structure and the proposed pilot stage.

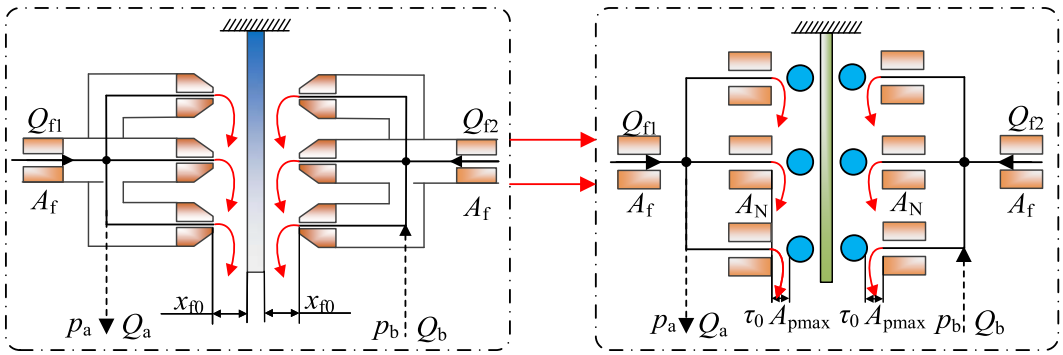

written as (Zhu et al. 2015)

$$Q_{ma} = Q_{pf1} - 3Q_{ha} = C_{pf}A_{pf}\sqrt{\frac{2(p_s - p_{ma})}{\rho}} - 3C_hA_{hmax}(\tau_0 - \tau)\sqrt{\frac{2p_{ma}}{\rho}} \tag{12}$$

$$Q_{mb} = 3Q_{hb} - Q_{pf2} = 3C_hA_{hmax}(\tau_0+\tau)\sqrt{\frac{2p_{mb}}{\rho}} - C_{pf}A_{pf}\sqrt{\frac{2(p_s - p_{mb})}{\rho}} \tag{13}$$

where τ_0 and τ are the original duty cycle and control duty cycle of the digital pilot PWM signal, respectively.

When the load is cutoff, the pressure characteristic can be defined as

$$\frac{p_{ma}}{p_s} = \left[1+\left(\frac{3C_hA_{hmax}(\tau_0 - \tau)}{C_{pf}A_{pf}}\right)^2\right]^{-1} \tag{14}$$

Letting

$$a = \frac{C_hA_{hmax}\tau_0}{C_{pf}A_{pf}} \tag{15}$$

Then eq. 14 is re-written as

$$\frac{p_{ma}}{p_s} = \left[1+a^2\left(1 - \frac{\tau}{\tau_0}\right)^2\right]^{-1} \tag{16}$$

The pressure sensitivity at the initial position of the digital pilot stage is written as

$$\frac{dp_{ma}}{d\tau}|_{\tau=0} = \frac{p_s}{\tau_0}\frac{18a^2}{(1+9a^2)^2} \tag{17}$$

The maximum pressure sensitivity is obtained when the following equation is satisfied:

$$\frac{d}{da}\left(\frac{dp_s}{d\tau}|_{\tau=0}\right) = \frac{p_s}{\tau_0}\frac{36a(1-9a^2)}{(1+9a^2)^3} \tag{18}$$

That is, the following conditions are met

$$a = \frac{C_hA_{hmax}\tau_0}{C_{pf}\pi d_{pf}^2/4} = \frac{1}{3} \tag{19}$$

Then, the diameter of the orifice is calculated by

$$d_{pf} = 2\sqrt{\frac{3C_hA_{hmax}\tau_0}{C_{pf}\pi}} \tag{20}$$

According to eq. 20, the original duty cycle τ_0 is the key to calculate the orifice diameter. To achieve the original duty cycle, a design method considering the flow controllability and flow linearization is given. To avoid flow saturation of the pilot stage, the following equation is given (Merritt 1978):

$$A_{hmax}\tau_0 \le \frac{1}{4}A_n = \frac{1}{16}\pi d_n^2 \tag{21}$$

where A_n and d_n are the nozzle's area (equal to the flow area of seat hole) and the nozzle's diameter (equal to the diameter of valve seat's hole).

Fig. 9. Normalized flow characteristic of the high-speed on/off valve.

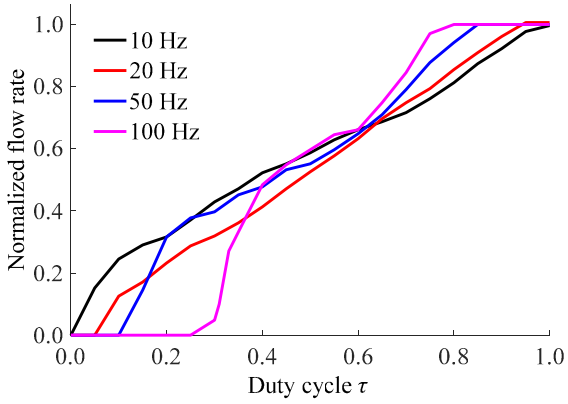

According to eq. 21, the digital pilot stage can achieve good flow controllability when the original duty cycle satisfies the following conditions:

$$\tau_0 \le 0.334 \tag{22}$$

However, in addition to considering the problem of avoiding the flow saturation of the digital pilot stage, it is also necessary to consider the linearity of the pilot HSV output flow of the pilot. When pilot HSV works in switching mode, the static flow consists of a dead zone (small duty cycle), a linear zone, and saturation (large duty cycle). Where in the linear region, the slope of the pilot HSV static flow curve (flow-to-duty cycle derivation) can be written as

$$\frac{\partial Q_h}{\partial \tau} = fQ_{hmax}\frac{\partial t_{on}}{\partial \tau} = Q_{hmax},\ t_{ton} < \frac{\tau}{f} \le \frac{1}{f} - t_{toff} \tag{23}$$

where Q_h and Q_{hmax} denote the flow rate and maximum flow rate of the HSV, respectively, and f denotes the PWM signal frequency.

According to eq. 23, in linear region (t_{ton}, $1/f$–t_{toff}), the output flow rate of the pilot HSV has a linear relationship with the input duty cycle. As the PWM frequency increases, the linear region gradually decreases, but the middle position of the linear region still maintains good linearity. And the duty cycle at the middle position is written as

$$\tau_m = \frac{T - t_{toff} + t_{ton}}{2T} = 0.5 + \frac{t_{ton} - t_{toff}}{2T} \tag{24}$$

where τ_m denotes the duty cycle at the middle position in the linear region.

The adaptive PWM signal is usually used to drive pilot HSV to get high dynamic performance that a pre-existing voltage is designed to improve the opening dynamic performance (Zhong et al. 2021) and a negative voltage signal is applied to coil to accelerate demagnetization during the closing stage (Zhang et al. 2018; Gao et al. 2020). Then the value of t_{toff} decreases and is closer to t_{ton}, which leads to that τ_m is approximately 0.5. The experimenters of the normalized static flow rate are shown in Fig. 9.

It can be seen from Fig. 9 that when the frequency is lower than 100 Hz, the output flow rate of the HSV is able to maintain good linearity between the duty cycle of 0.2–0.8; therefore, the duty cycle calculated by eq. 22 can be selected. How-

Fig. 10. Optimized simulation results of the proposed d_f.

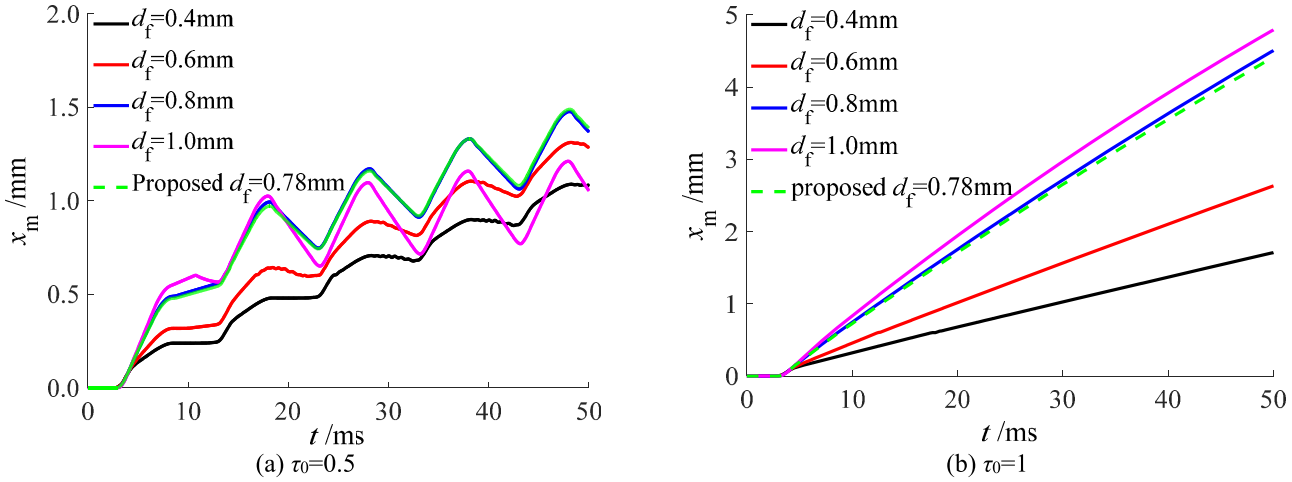

Fig. 11. Proportional valve performance test platform schematic diagram. HSV, high-speed on/off valve; HSVA, high- peed on/off valve array.

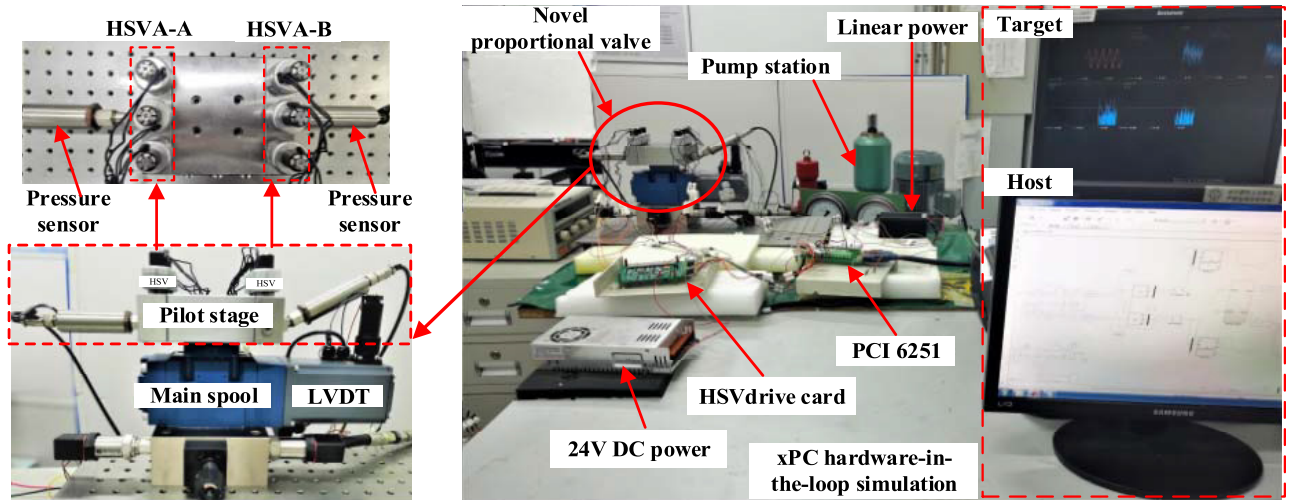

ever, in this study, to ensure the control accuracy, 100 Hz is selected as the switching frequency of the HSV, and the HSV is almost unable to output the flow when the duty cycle is 0.334. Therefore, priority can only be given to ensuring flow linearity with a duty cycle of 0.5.

In conclusion, according to eq. 20, the actual value of the pilot orifice's diameter is calculated by

$$d_{pf} = \sqrt{\frac{6C_h A_{hmax}}{C_{pf}\pi}} = 0.78 \quad (25)$$

4.3. Simulation verification of the design method

To verify the feasibility of the design method, lots of simulations are carried out as shown in Fig. 10.

Figure 10 indicates that, with the proposed design method, a better balance between the displacement fluctuation and dynamic performance of the main spool is obtained. Therefore, considering the actual processing difficulty, the fixed orifice with 0.8 mm diameter standard is selected as the study object.

5. Experimental study

A hydraulic test platform is established to analyze the comprehensive performance of the HFTSPV, as shown in Fig. 11.

The platform is composed of a hydraulic pump station, an xPC hardware-in-the-loop simulation (xPC HILS) system, and the proposed HFTSPV prototype. The maximum working pressure of the HSVA is 10 MPa, and the main spool stage used in this study is same as reference Gao et al. (2021). The working pressure of the pilot stage is set to be 4 MPa by pressure reducing valve. The xPC HILS system consists of a host computer, an industrial computer, and a data acquisition card (PCI 6251). PWM signals are generated in MATLAB/Simulink to drive the HSVA. The data acquisition card is used to collect the main spool's position and pressure signals, and output PWM signal with 5 V. A commercial HSV drive card is used to amplify the low-voltage PWM signal into high-voltage PWM signal.

Fig. 12. Influences of fixed orifice's diameter on the dynamic characteristics of main spool.

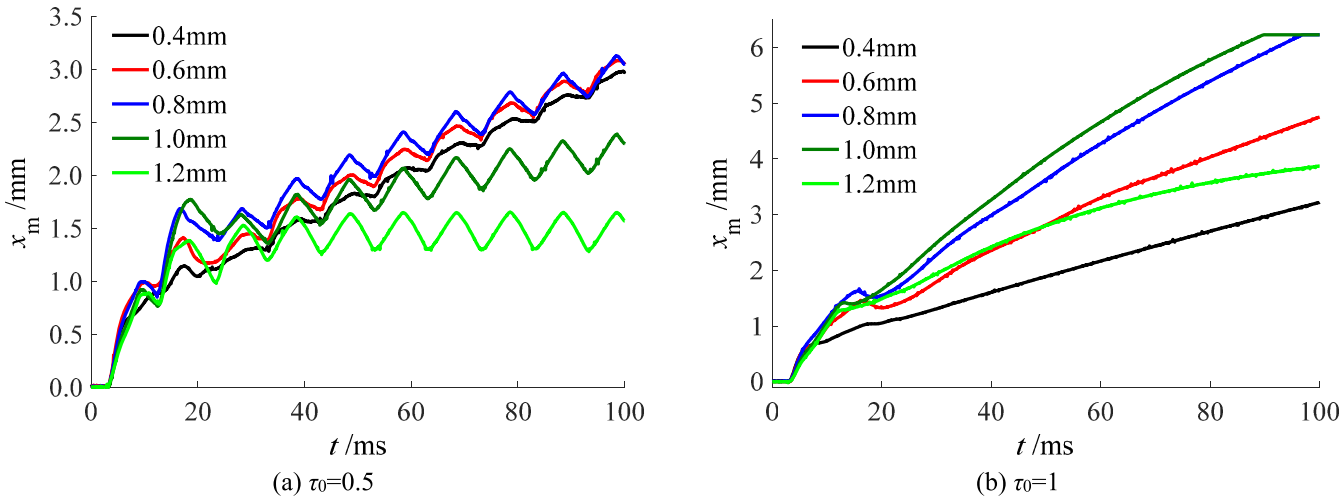

(a) τ_0=0.5 (b) τ_0=1

Fig. 13. Displacement step tracking performance of the proposed high-frequency two-stage proportional valve.

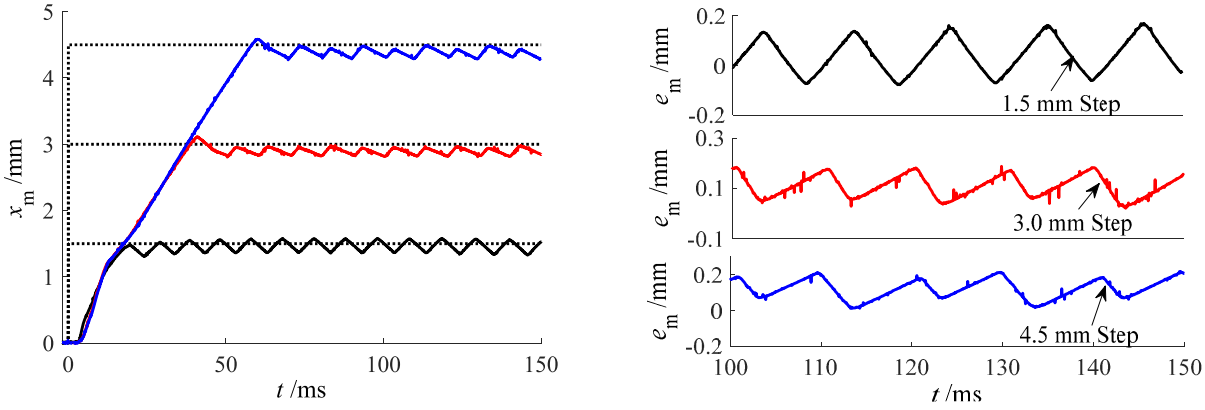

(a) step tracking performance (b) steady tracking error

5.1. Influences of the orifice's diameter

The influence of fixed orifice's diameters on the dynamic characteristics of the main spool is shown in Fig. 12. In the figure, the frequency and duty cycle of the PWM control signal are set to 100 Hz and 0.5, respectively.

As exhibited in Fig. 12, when the duty cycle is 0.5, with the increase of the fixed orifice's diameter, the oscillation amplitude of the main spool's displacement increases, which causes the displacement to decrease during certain period. When the duty cycle is 1, as the fixed orifice's diameter increases, the dynamic performance of the main spool first increases and then decreases. When using the proposed fixed orifice's diameter with 0.8 mm diameter standard, a compromise between the displacement oscillation and dynamic performance of the main spool are obtained simultaneously, which proves the effectiveness of the proposed design method of the orifice's diameter.

5.2. Step tracking performance

As shown in Fig. 13, the experimental results of the main valve core tracking different displacement steps are shown. In the figure, the reference step signal is 3 mm, and the switching frequency of HSV is selected as 100 Hz.

It can be seen from Fig. 13 that the delay time of the proposed HFTSPV always maintains within 3.3 ms under different command signals, which is mainly affected by the dynamic characteristics of the pilot HSVA. The maximum overshoot and maximum steady error of the displacement tracking results are 0.113 mm and 0.211 mm, which can be further reduced by increasing the switching frequency of the pilot HSVA. In addition, the rising times of the proposed HFTSPV under different reference tracking signals are 16.2, 34.5, and 50.2 ms, respectively, which relates to the maximum output flow rate of the pilot HSVA.

5.3. Sinusoidal tracking performance

Comparisons of the sinusoidal tracking performance between the proposed HFTSPV and the traditional valve are shown in Fig. 14.

It can be seen from Fig. 14 that the proposed HFTSPV can track the displacement of different sinusoidal signals under the PID closed-loop control strategy. However, when track-

Fig. 14. Comparisons of displacement sinusoidal tracking between the proposed high-frequency two-stage proportional valve and the traditional valve.

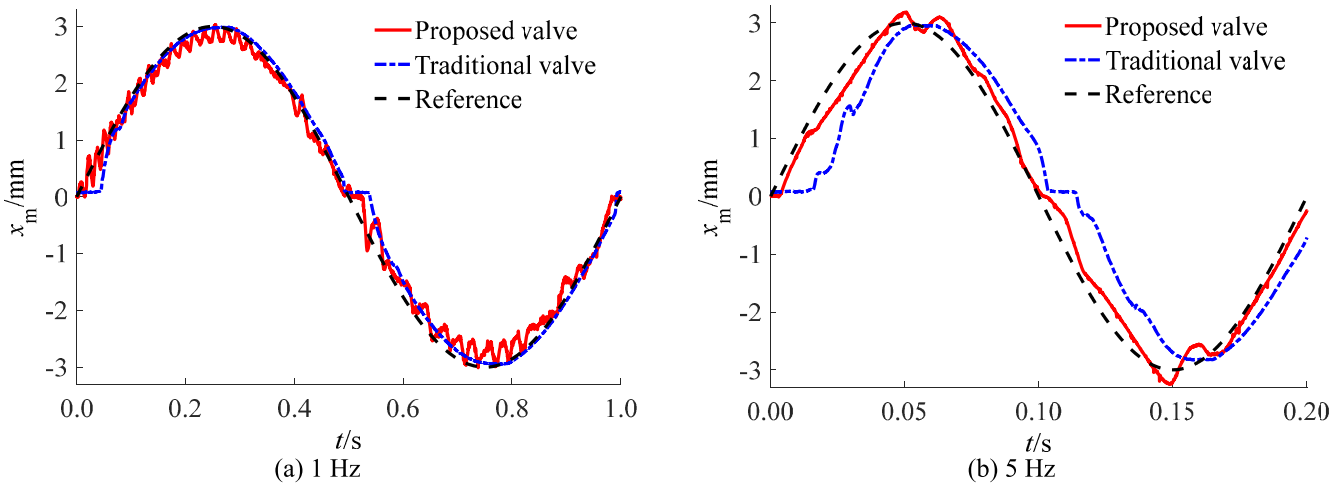

Table 2. Comparisons of the displacement sinusoidal tracking.

Sinusoid tracking	Valve type	M_e (mm)	μ (mm)	σ (mm)
Signal 1 (frequency is 1 Hz)	Traditional TSPV	0.770	0.137	0.194
	Proposed HFTSPV	0.600 (↓22.1%)	0.166 (↑21.2%)	0.201 (↑3.6%)
Signal 2 (frequency is 5 Hz)	Traditional TSPV	1.427	0.599	0.710
	Proposed HFTSPV	0.544 (↓61.9%)	0.218 (↓63.6%)	0.249 (↓64.9%)

Note: TSPV, two-stage proportional valves; HFTSPV, high-frequency two-stage proportional valve.

ing the sinusoidal signal with 1 Hz, the tracking error of the HFTSPV is slightly bigger than that of the traditional TSPV, due to the displacement fluctuations caused by the discrete flow rate of the HSVA. When the pilot HSVA works in high-frequency switching state, the pressure in the control chamber of the main spool oscillates, which leads to the motion oscillation of the main spool under the joint action of the hydraulic pressure in the control chamber and spring force. When tracking the sinusoidal signal with 5 Hz, the switching times of the HSVA are smaller than that of HSVA when tracking the sinusoidal signal with 1 Hz, which leads to the smaller displacement fluctuations. Since the pilot HSVA has no structural dead zone, the tracking performance of the HFTSPV is better than that of the traditional TSPV.

Comparisons of the displacement tracking indexes between the proposed HFTSPV and traditional TSPV are presented in Table 2, where M_e denotes the maximum error, μ denotes the average error, and σ denotes the standard deviation of the tracking error (Yao et al. 2015).

Tracking results shown in Table 2 show that, compared to the traditional valve, when tracking a sinusoidal signal with a frequency of 1 Hz, the high-frequency switching of the digital pilot stage causes fluctuations in the transmission displacement, which increases the average error and the error standard deviation by 21.2% and 3.6%, respectively, but the maximum error is reduced by 22.1%. Conversely, with the increase of tracking frequency, the maximum error, average error, and standard deviation of the proposed HFTSPV's displacement tracking are reduced by 61.9%, 63.6%, and 64.9%, respectively. Therefore, it is necessary to further study the high precision control strategy to improve the control precision of the proposed HFTSPV.

5.4. Amplitude–frequency characteristic of HFTSPV

During experiment, the position data of the proposed HFTSPV is only collected by LVDT sensor, the amplitude–frequency characteristic experiments should be carried out based on closed-loop control mode. First, the sinusoidal signal is selected as the command, and its amplitude is set to ±50% full stroke or 0%–50% full stroke of the main spool. Second, increasing the tracking frequency until the amplitude of the displacement data are reduced by 60%. Finally, the amplitude–frequency characteristics of HFTSPV are obtained by converting the time-domain data to the frequency-domain data of the displacement through Laplace transform method, as shown in Fig. 15.

As exhibited in Fig. 15, under the condition of ±50% maximum spool displacement, the −3 dB frequency of HFTSPV reaches 16 Hz, while it reaches 30 Hz under the condition of 0%–50% full scale. In contrast to the traditional TSPV (15 Hz@±50% full scale and 25 Hz@ 0–50% full scale), the proposed HFTSPV has better amplitude–frequency performance. However, compared to the previous valve (9.5 Hz@±50% full scale and 15 Hz@ 0–50% full scale) designed by our research lab (Gao et al. 2021), the amplitude–frequency characteristics are significantly improved. This is because the proposed pilot HSVA consists of three HSVs in parallel, which simultane-

Fig. 15. Amplitude–frequency characteristics of the proposed high-frequency two-stage proportional valve.

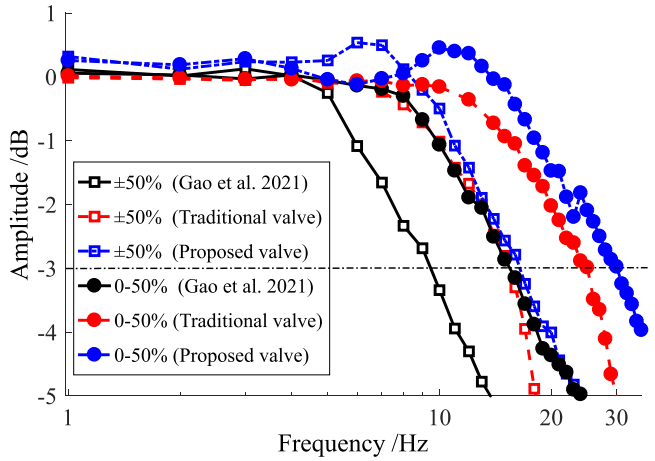

ously realizes the big flow rate and the good dynamic performance.

6. Conclusions

A novel HFTSPV piloted by two HSVAs is proposed according to the dual nozzle flapper structure characteristic, and it fully integrates the advantages of parallel-connected digital valve technology. The important conclusions are summarized as follows:

(1) The influences of the fixed orifice's diameter on the moving characteristics of the main spool are analyzed by lost of simulations under the conditions of different duty cycles. The results show that when the diameter of the orifice is in the range of 0.4–1.0 mm, as the diameter gradually increases, the flow rate into the control chamber increases, which leads to the increase of the main spool's displacement. However, when the orifice's diameter reaches 1.2 mm, the throttling effect of the orifice is very small, which causes the pressure in the control chamber to be close to the pilot supply pressure, therefore the moving speed of the main spool is reduced.

(2) Inspired by the design method of the dual nozzle flapper structure, a design criterion of the orifice's diameter is proposed based on maximum pressure sensitivity and flow linearization of the pilot HSV. Simulation and experimental results indicate that a good compromise between displacement fluctuation and dynamic performance of the main spool is obtained by the proposed design criterion.

(3) Different step displacement tracking experiments show that the opening delay time of the proposed HFTSPV is closed to 3.3 ms, the maximum overshoot and the maximum steady-state error are 0.113 and 0.211 mm, respectively. In addition, the tracking error of the proposed HFTSPV is slightly larger than that of the traditional TSPV when tracking the sinusoidal signal with 1 Hz, and smaller than that of the traditional TSPV when tracking the sinusoidal signal with 5 Hz. This is because that the displacement fluctuations caused by the discrete flow rate of the pilot HSVA is bigger especially in low tracking frequency.

(4) The amplitude–frequency characteristics of the proposed HFTSPV were experimentally obtained. The results showed that the cutoff frequency at −3 dB was 16 Hz under the ±50% full-scale amplitude tracking signal, and the cutoff frequency reached 30 Hz under the 0%–50% full-scale condition, which was much higher than that of the traditional TSPV (15 Hz@±50% full-scale and 25 Hz@0(50% full-scale).

In the future, it is necessary to further study the high precision displacement control of the HFTSPV and the optimal switching strategy of the pilot HSVA to fulfill the minimum switching times.

Acknowledgements

This work was supported by the National Natural Science Foundation of China (52375059) and the Fundamental Research Funds for the Central Universities (NO.NP2022305).

Article information

History dates

Received: 24 April 2024
Accepted: 3 July 2024
Accepted manuscript online: 13 September 2024
Version of record online: 8 October 2024

Copyright

Data availability

Data generated or analyzed during this study are available from the corresponding author upon reasonable request.

Author information

Author ORCIDs

Qiang Gao https://orcid.org/0000-0002-9318-4501
Linfei Li https://orcid.org/0009-0003-4583-5589

Author contributions

Conceptualization: QG, LL
Data curation: QG, LL
Formal analysis: LL
Funding acquisition: QG, YZ
Investigation: QG
Methodology: YZ
Project administration: QG, YZ
Resources: QG
Software: LL
Validation: LL

Visualization: QG
Writing – review & editing: YZ

Competing interests

The authors declare there are no competing interests.

References

Brandstetter, R., Deubel, T., Scheidl, R., Winkler, B., and Zeman, K. 2017. Digital hydraulics and "Industrie 4.0." Proc. Inst. Mech. Eng. Part I J. Syst. Control Eng. **231**(2): 82–93. doi:10.1177/0959651816636734.

Gao, Q., Lan, B., and Zhu, Y. 2024. Modelling and characteristics analysis of an electro-hydraulic proportional valve with a discrete pilot stage for underwater hydraulic manipulators. Proc. Inst. Mech. Eng. Part C J. Eng. Mech. Eng. Sci. doi:10.1177/09544062241230176.

Gao, Q., Zhu, Y., and Liu, J.H. 2022. Dynamics modelling and control of a novel fuel metering valve actuated by two binary-coded digital valve arrays. Machines, **10**(1): 55. doi:10.3390/machines10010055.

Gao, Q., Zhu, Y.C., Luo., Z., and Bruno, N. 2020. Investigation on adaptive pulse width modulation control for high speed on off valve. J. Mech. Sci. Technol. **34**(4): 1711–1722. doi:10.1007/s12206-020-0333-y.

Gao, Q., Zhu, Y.C., Wu, C.W., and Jiang, Y.L. 2021. Development of a novel two-stage proportional valve with a pilot digital flow distribution. Front. Mech. Eng. **16**(2): 420–434. doi:10.1007/s11465-020-0622-2.

Hou, J.Y., Zhang, Z.M., Ning, D.Y., and Gong, Y.J. 2017. Model-based position tracking control of a hose-connected hydraulic lifting system. Flow Meas. Instrum. **53**: 286–292. doi:10.1016/j.flowmeasinst.2016.08.001.

Laamanen, A., Linjama, M., and Vilenius, M. 2003. Characteristics of a Digital Flow Control Unit with PCM control. *In* Seventh Triennial International Symposium on Fluid Control, Measurement and Visualization, August 25–28, Sorrento, Italy, CD-ROM Proceedings. ISBN 0-9533991-4-1.

Lantela, T., and Pietola, M. 2017. High-flow rate miniature digital valve system. Int. J. Fluid Power, **18**(3): 188–195. doi:10.1080/14399776.2017.1358025.

Li, R.J., Shang, Y.X., Liu, X.C., Wu, S., and Qi, P.Y. 2023. Antidisturbance slip ratio algorithm of aircraft braking system based on on/off valves. J. Aircr. **61**(1): 116–127. doi:10.2514/1.C037438.

Merritt, H.E. 1978. Hydraulic control systems (in Chinese, trans. Chen Yanqing). Science Press, Beijing. pp. 97–104. (Original work published 1967).

Nie, S.L., Liu, X.Y., Yin, F.L., Ji, H., and Zhang, J.X. 2018. Development of a high-pressure pneumatic on/off valve with high transient performances direct-driven by voice coil motor. Appl. Sci. Basel, **8**(4): 611. doi:10.3390/app8040611.

Paloniitty, M. 2018. Novel water hydraulic on/off valves and tracking control method for equal coded valve system. Dissertation for the Doctoral Degree. Tampere University of Technology, Tampere. pp. 54–55.

Paloniitty, M., and Linjama, M. 2018. High-linear digital hydraulic valve control by an equal coded valve system and novel switching schemes. Proc. Inst. Mech. Eng. Part I J. Syst. Control Eng. **232**(3): 258–269. doi:10.1177/0959651817750519.

Pan, M., and Plummer, A. 2018. Digital switched hydraulics. Front. Mech. Eng. **13**(2): 225–231. doi:10.1007/s11465-018-0509-7.

Tamburrano, P., Plummer, A.R., De, P.P., Distaso, E., and Amirante, R. 2020. A novel servo valve pilot stage actuated by a piezoelectric ring bender (Part II): design model and full simulation. Energies, **13**: 2267. doi:10.3390/en13092267.

Wang, H., Wang, X.H., Huang, J.H., and Quan, L. 2020. Flow control for a two-stage proportional valve with hydraulic position feedback. Chin. J. Mech. Eng. **33**(1): 1–13. doi:10.1186/s10033-020-00517-4.

Wang, H., Wang, X.H., Huang, J.H., and Quan, L. 2021. Performance improvement of a two-stage proportional valve with internal hydraulic position feedback. J. Dyn. Syst. Meas. Control Trans. ASME, **143**(7): 1–9. doi:10.1115/1.4049793.

Wang, P., Cheng, Y.W., Linjama, M., Yao, J., and Shan, D.S. 2023. A novel equivalent continuous metering control with a uniform switching strategy for digital valve system. IEEE-ASME Trans. Mechatron. **28**(5): 2449–2460. doi:10.1109/TMECH.2023.3247220.

Xiong, X.Y., and Huang, J.H. 2018. Performance of a flow control valve with pilot switching valve. Proc. Inst. Mech. Eng. Part I J. Syst. Control Eng. **232**(2): 178–194. doi:10.1177/0959651817743889.

Xu, B., Su, Q., Zhang, J.H., and Lu, Z.Y. 2016. A dead-band model and its online detection for the pilot stage of a two-stage directional flow control valve. Proc. Inst. Mech. Eng. Part C J. Eng. Mech. Eng. Sci. **230**(4): 639–654. doi:10.1177/0954406215578158.

Xu, B., Su, Q., Zhang, J.H., and Lu, Z.Y. 2017. Analysis and compensation for the cascade dead-zones in the proportional control valve. ISA Trans. **66**: 393–403. doi:10.1016/j.isatra.2016.10.012.

Yang, H.Y., and Pan, M. 2015. Engineering research in fluid power: a review. J. Zhejiang Univ. Sci. A, **16**(6): 427–442. doi:10.1631/jzus.A1500042.

Yao, J.Y., Deng, W.X., and Jiao, Z.X. 2015. Adaptive control of hydraulic actuators with LuGre model-based friction compensation. IEEE Trans. Ind. Electron. **62**(10): 6469–6477. doi:10.1109/TIE.2015.2423660.

Yin, Y., Nie, H., Ni, H.J., and Zhang, M. 2016. Reliability analysis of landing gear retraction system influenced by multifactors. J. Aircr. **53**(3): 713–724. doi:10.2514/1.C033333.

Zeng, Y.S., Wang, D.M., Zi, B., and Zeng, Q. 2015. Dynamic characteristics of priority control system for high-speed on-off digital valve. Adv. Mech. Eng. **7**(4): 1–8. doi:10.1177/1687814015582098.

Zhang, B., Zhong, Q., Ma, J.E., Hong, H.C., Bao, H.M., Shi, Y., and Yang, H.Y. 2018. Self-correcting PWM control for dynamic performance preservation in high speed on/off valve. Mechatronics, **55**: 141–150. doi:10.1016/j.mechatronics.2018.09.001.

Zhang, H., Zhao, J.Y., and Wang, Y.F. 2023. Research on high water-based digital valve with dual-spool and control strategy. Proc. Inst. Mech. Eng. Part E J. Process Mech. Eng. **238**(2): 819–836. doi:10.1177/09544089231174285.

Zhang, J.H., Lu, Z.Y., Xu, B., and Su, Q. 2019. Investigation on the dynamic characteristics and control accuracy of a novel proportional directional valve with independently controlled pilot stage. ISA Trans. **93**: 218–230. doi:10.1016/j.isatra.2019.03.023.

Zhong, Q., Bao, H.M., Li, Y.B., Hong, H.C., Zhang, B., and Yang, H.Y. 2021. Investigation into the independent metering control performance of a twin spools valve with switching technology-controlled pilot stage. Chin. J. Mech. Eng. **34**(1): 1–17. doi:10.1186/s10033-021-00616-w.

Zhong, Q., Wang, X.L., Xie, G., Yang, H.Y., Yu, C., Xu, E.G., and Li, Y.B. 2021. Analysis of dynamic characteristics and power losses of high speed on /off valve with pre-existing control algorithm. Energies, **14**(16): 4901–4912. doi:10.3390/en14164901.

Zhong, Q., Xu, E.G., Jia, T.W., Yang, H.Y., Zhang, B., and Li, Y.B. 2022. Dynamic performance and control accuracy of a novel proportional valve with a switching technology-controlled pilot stage. J. Zhejiang Univ. Sci. A, **23**(4): 272–285. doi:10.1631/jzus.A2100463.

Zhu, Y.C., Yang, X.L., and Wang, X.L. 2015. Development of a four-nozzle flapper servovalve driven by a giant magnetostrictive actuator. Proc. Inst. Mech. Eng. Part I J. Syst. Control Eng. **229**(4): 293–307. doi:10.1177/0959651814565829.